


 Cite this: *RSC Adv.*, 2019, 9, 15061

Preparation, characterization, and use of novel Cu@Fe₃O₄ MNPs in the synthesis of tetrahydrobenzimidazo[2,1-*b*]quinazolin-1(2*H*)-ones and 2*H*-indazolo[2,1-*b*]phthalazine-triones under solvent-free conditions†

 Lilin Jiang^a and Zumrat Druzhinin *^b

Cu@Fe₃O₄ MNPs as novel nanomagnetic reagents were prepared to investigate their catalytic behavior in the preparation of tetrahydrobenzimidazo[2,1-*b*]quinazolin-1(2*H*)-ones, as important biologically active compounds. Then, characterization of the synthesized nanoparticles was performed using different methods including Fourier transform infrared spectroscopy (FT-IR), X-ray diffraction (XRD) analysis, thermogravimetric analysis (TGA), vibrating sample magnetometer (VSM), energy dispersive X-ray (EDX), and scanning electron microscopy (SEM). All reactions were performed with small amounts of the Cu@Fe₃O₄ MNPs under solvent-free conditions. After completion of the reaction, because of the magnetic nature of the nanocatalyst, they could be simply separated with an external magnet and easily reused with no considerable decrease in the catalytic behavior even after seven runs.

Received 27th February 2019

Accepted 7th May 2019

DOI: 10.1039/c9ra01509d

rsc.li/rsc-advances

Introduction

The use of eco-friendly, efficient, and maintainable reusable heterogeneous magnetic nanocatalysts involves both economic and ecological advantages.¹ Coating of iron oxides with silica to form core-shell structures is considered a good semi-heterogeneous catalyst owing to the existence of surface FeOH groups. These groups in magnetic nanoparticles, as beneficial groups for the immobilization of homogeneous catalysts, are among the main issues in organic transformations. Among the noticeable characteristics of these nanoparticles are their high specific surface area and easy separation from the solution using an appropriate permanent magnet compared with centrifugation or filtration, which are not convenient for small magnetic nanoparticles.^{2–8}

Heterocyclic compounds have attracted extensive attention in the field of chemical research because of their striking structural features, clinical applications, and pharmacological properties. Recently, the preparation of quinazolinone derivatives has been of extensive interest because of their biological and pharmaceutical activities such as antihypertensive, anti-histaminic, analgesic and anti-inflammatory, anticancer, and anti-HIV.^{9–13} In chemistry, compounds with the quinazolinone

skeleton such as tetrahydrobenzimidazo[2,1-*b*]quinazolin-1(2*H*)-ones have been widely utilized as building blocks in plenty of natural and synthetic products. In order to synthesize tetrahydrobenzimidazo[2,1-*b*]quinazolin-1(2*H*)-ones, a variety of strategies have been developed in the recent studies. However, these techniques suffer from some drawbacks such as long reaction times, requiring a large amount of the catalyst, and difficulty in catalyst isolation from the solution.^{14–18} Therefore, the search for improving reaction conditions for the preparation of these kinds of heterocyclic molecules *via* the three-component reaction between 2-aminobenzimidazole, aldehyde, and 5,5-dimethyl-1,3-cyclohexanedione using effective and recoverable catalysts under green conditions is a prime and real challenge for synthetic chemists.

The molecules containing phthalhydrazide moiety such as 2*H*-indazolo[2,1-*b*]phthalazine-triones has wide pharmaceutical and biological activities, such as anticonvulsant, cardiostonic, antifungal, anticancer, and vasorelaxant properties.^{19–23} Diverse types of method and catalyst have been developed for the acceleration of the production of phthalazine derivatives; however, several of these procedures suffer from some limitations.^{24–30} Hence, it is essential to expand an improved path for the effectual synthesis of these compounds under mild reaction conditions.

Experimental

General

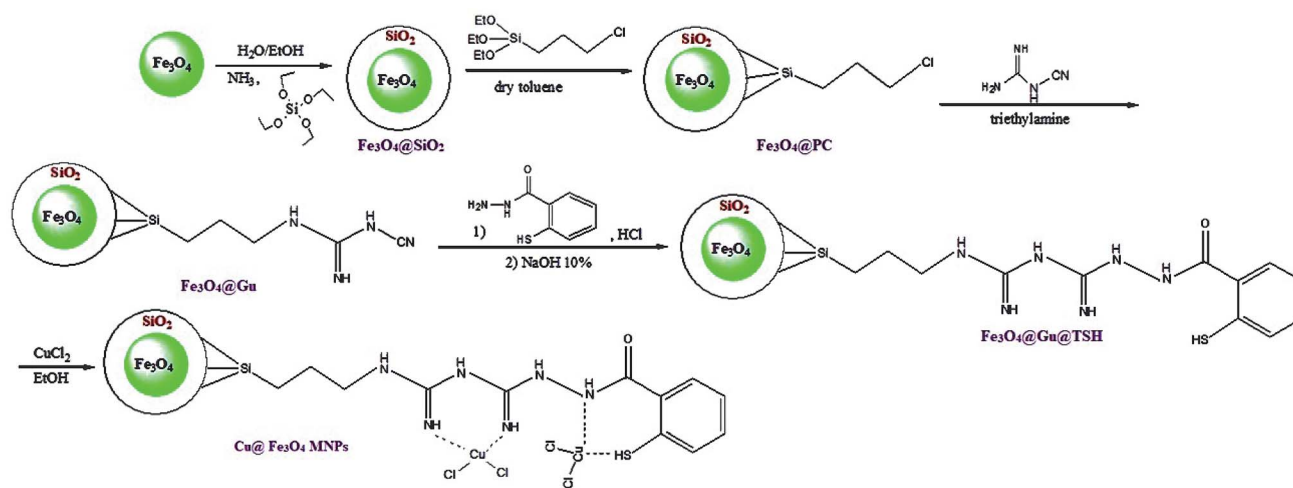
All the pure substances were prepared from Merck, Aldrich, and Fluka chemical companies. Melting points of the substrate were

^aSchool of Information and Communication Engineering, Hezhou University, Hezhou, 542899, China

^bTajik Technical University, Tajikistan. E-mail: zumratdruzhinin@gmail.com

† Electronic supplementary information (ESI) available. See DOI: 10.1039/c9ra01509d





Scheme 1 All stages of the Cu@Fe₃O₄ MNPs synthesis.

determined using an Electrothermal-9100 apparatus with no correction. FT-IR spectroscopy was performed using a PerkinElmer PXI spectrometer in KBr wafers. TGA spectra were obtained using a TGA thermoanalyzer (PerkinElmer) instrument. The chemical composition was determined by means of energy dispersive X-ray spectroscopy (EDX) (ESEM, Philips, and XL30). The X-ray diffraction (XRD) measurements of catalyst were carried out with a Siemens D-500 X-ray diffractometer (Munich, Germany). Scanning electron microscopy was performed using an SEM-LEO 1430VP analyzer. Magnetic susceptibility measurements were accomplished using vibrating sample magnetometry (VSM; Lake Shore 7200 at 300 K VSM).

Catalyst synthesis

Preparation of Fe₃O₄. Magnetic nanoparticles Fe₃O₄ were synthesized in accordance with the reported chemical co-precipitating Fe²⁺ and Fe³⁺ ions in the existence of ammonia solution. For this purpose, 2 g of FeCl₂·4H₂O and 5.4 g of FeCl₃·6H₂O were dissolved in 40 mL deoxygenated water containing 0.9 mL of concentrated HCl under a continuous flow of nitrogen gas. Black sediment was achieved by addition of 250 mL of NaOH solution into Fe²⁺ and Fe³⁺ solution at ambient temperature under agitation. After this time, the precipitate was magnetically isolated and washed several times with water and

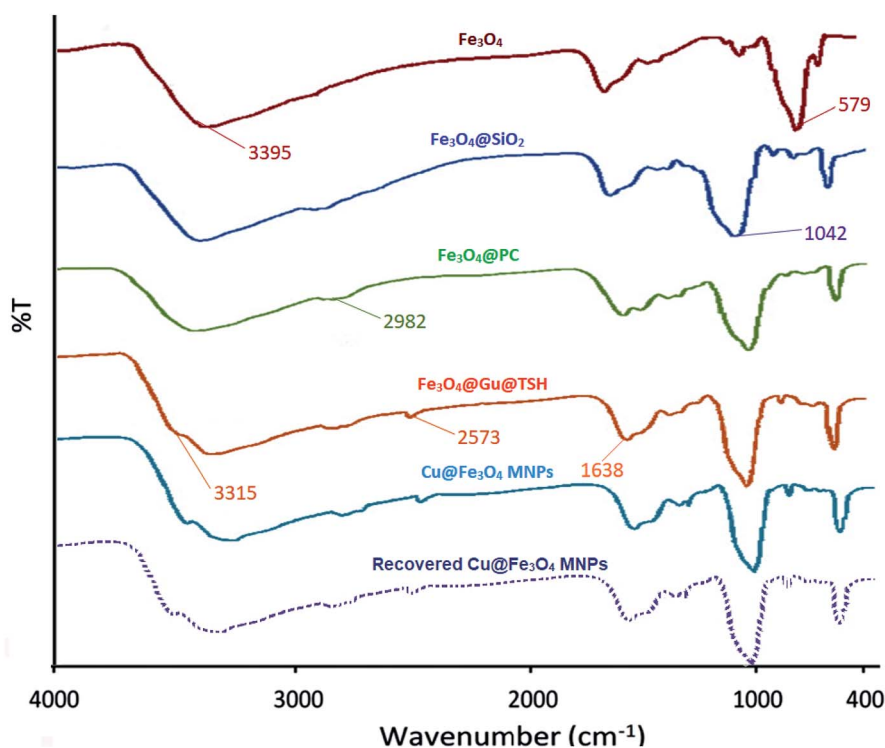
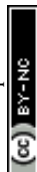


Fig. 1 FTIR spectra corresponding to Fe₃O₄, Fe₃O₄@SiO₂, Fe₃O₄@PC, Fe₃O₄@Gu@TSH, and Cu@Fe₃O₄ MNPs.



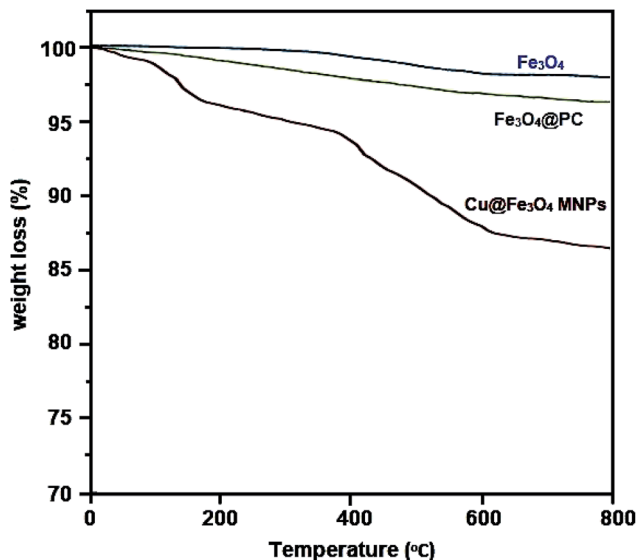


Fig. 2 TGA curves of Fe_3O_4 , $\text{Fe}_3\text{O}_4@\text{PC}$, and $\text{Cu}@\text{Fe}_3\text{O}_4$ MNPs.

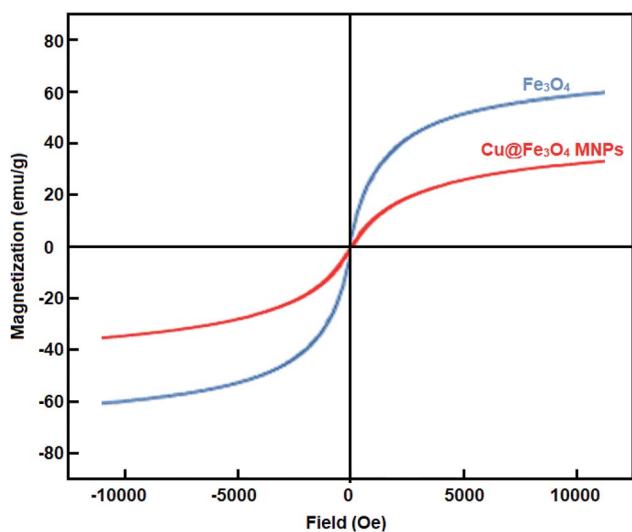


Fig. 3 VSM magnetization curves corresponding to the bare Fe_3O_4 and $\text{Cu}@\text{Fe}_3\text{O}_4$ MNPs.

ethanol. Finally, the precipitate was dried at 40 °C for 24 h and stored in glass vials.

Preparation of $\text{Fe}_3\text{O}_4@\text{SiO}_2$. About 1 g of the Fe_3O_4 was dispersed in a mixture of EtOH (40 mL) and deionized water (5 mL) by ultrasonication for 20 min, followed by the addition of 3 mL of aqueous ammonia (28 wt%) and 0.5 mL of triethoxysilane (TEOS). The obtained mixture was mechanically stirred at 400 rpm for 24 h at 25 °C. After completion of the reaction, the precipitates of core-shell $\text{Fe}_3\text{O}_4@\text{SiO}_2$ nanoparticles were collected by magnetic separation, washed several times with diluted hydrochloric acid, and deionized water, and dried under vacuum oven at 70 °C for 5 h.

Preparation of Fe_3O_4 bonded propyl chloride ($\text{Fe}_3\text{O}_4@\text{PC}$). About, 1 g of $\text{Fe}_3\text{O}_4@\text{SiO}_2$ nanoparticles were suspended in 20 mL dry toluene and sonicated for 20 min in an ultrasonic

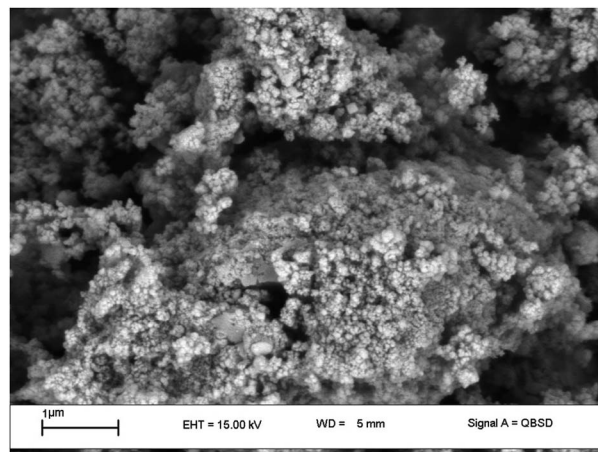


Fig. 4 SEM spectra of $\text{Cu}@\text{Fe}_3\text{O}_4$ MNPs.

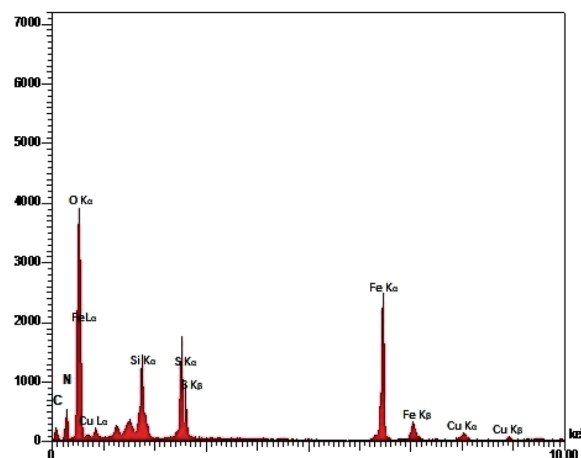


Fig. 5 EDX spectra of $\text{Cu}@\text{Fe}_3\text{O}_4$ MNPs.

bath. Then, 2 mL of 3-chloropropyltriethoxysilane (CPTCSi) was added into the flask and the reaction mixture was refluxed and mechanically agitated for 24 h under nitrogen atmosphere. At

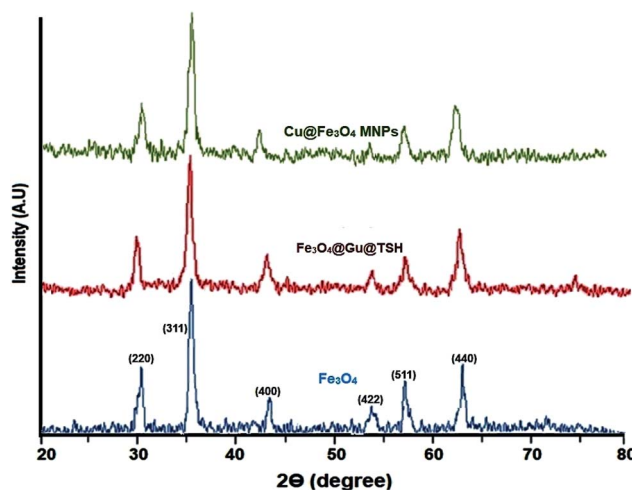
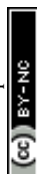
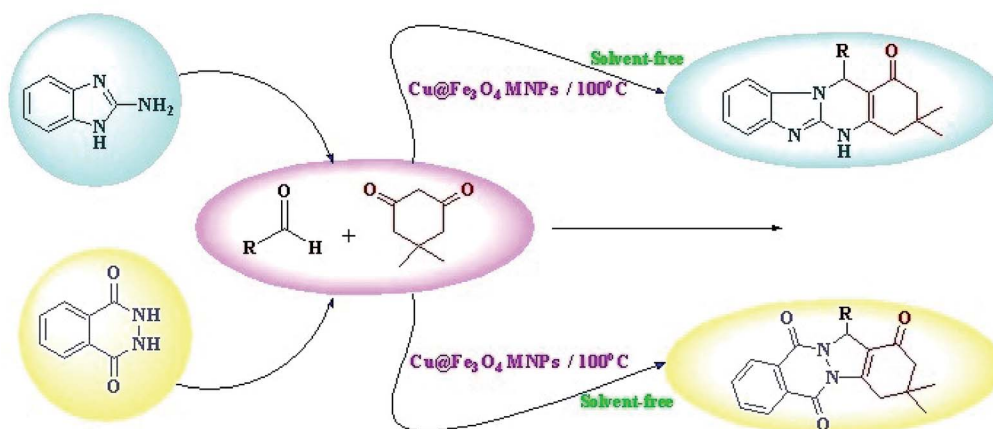


Fig. 6 The XRD patterns of Fe_3O_4 , $\text{Fe}_3\text{O}_4@\text{Gu}@\text{TSH}$ and $\text{Cu}@\text{Fe}_3\text{O}_4$ MNPs.





Scheme 2 Preparation of tetrahydrobenzimidazo[2,1-*b*]quinazolin-1(2*H*)-ones and 2*H*-indazolo[2,1-*b*]-phthalazine-triones using Cu@Fe₃O₄ MNPs.

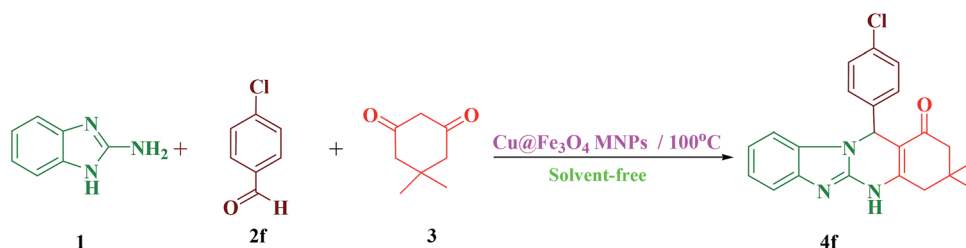
the end of the reaction, the suspension was collected using a powerful magnet and washed several times with ethanol and distilled water to remove any unreacted chemicals, and dried under vacuum oven.

Preparation of MNPs bonded dicyandiamide (Fe₃O₄@Gu). The MNPs@PC (2 g) was dispersed in 50 mL deionized water using ultrasonication for half an hour. Then, dicyandiamide (2 mmol) and triethylamine (1 mL) was poured in to the reaction vessel and refluxed for 2 h under a nitrogen atmosphere. After

this step, the resultant solid (MNPs@Gu) was isolated by a permanent magnet and rinsed with water and ethanol, and then dried under a vacuum oven.

Preparation of Fe₃O₄@Gu@TSH. First, 2 g of prepared MNPs@Gu was dissolved in 50 mL deionized water followed by a 30 min sonication. Then, 50 mL of thiosalicylhydrazide (0.05 M) along with 50 mL hydrochloric acid (0.15 M) was poured in to the reaction vessel and sonicated for 1 h. In the following reaction, the product was stirred with

Table 1 Optimization of the three-component reaction of 2-aminobenzimidazole (1), 4-chlorobenzaldehyde (2f), and dimedone (3) under various conditions^a



Entry	Solvent	Catalyst (mol%)	Temp.	Time (min)	Yield ^b (%)
1	CH ₃ CN	Cu@Fe ₃ O ₄ MNPs/0.38	Reflux	70	61
2	<i>n</i> -Hexane	Cu@Fe ₃ O ₄ MNPs/0.38	Reflux	120	Trace
3	H ₂ O	Cu@Fe ₃ O ₄ MNPs/0.38	Reflux	70	47
4	EtOH	Cu@Fe ₃ O ₄ MNPs/0.38	Reflux	60	64
5	Solvent-free	Cu@Fe ₃ O ₄ MNPs/0.38	25 °C	12	Trace
6	Solvent-free	Cu@Fe ₃ O ₄ MNPs/0.38	80 °C	12	83
7	Solvent-free	Cu@Fe ₃ O ₄ MNPs/0.38	90 °C	12	91
8	Solvent-free	Cu@Fe₃O₄ MNPs/0.38	100 °C	12	94
9	Solvent-free	Cu@Fe ₃ O ₄ MNPs/0.38	110 °C	12	92
10	Solvent-free	Cu@Fe ₃ O ₄ MNPs/0.19	100 °C	12	74
11	Solvent-free	Cu@Fe ₃ O ₄ MNPs/0.57	100 °C	12	93
12	Solvent-free	Fe ₃ O ₄ /0.38	100 °C	60	43
13	Solvent-free	Fe ₃ O ₄ @SiO ₂ /0.38	100 °C	55	51
14	Solvent-free	Fe ₃ O ₄ @PC/0.38	100 °C	50	59
15	Solvent-free	Fe ₃ O ₄ @Gu/0.38	100 °C	40	71
16	Solvent-free	Fe ₃ O ₄ @Gu@TSH/0.38	100 °C	25	83

^a Reaction conditions: 2-aminobenzimidazole (1 mmol), 4-chlorobenzaldehyde (1 mmol), dimedone (1 mmol), and required amount of the catalysts. ^b The yields refer to the isolated product.



Table 2 Cu@Fe₃O₄ MNPs-catalyzed synthesis of tetrahydrobenzimidazo[2,1-*b*]quinazolin-1(2*H*)-one (**4**) derivatives^a

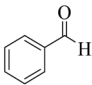
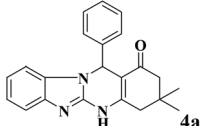
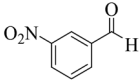
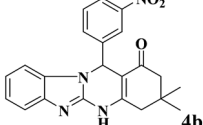
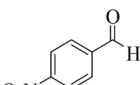
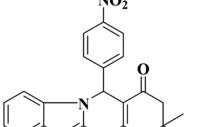
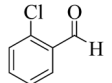
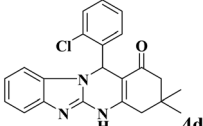
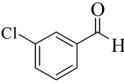
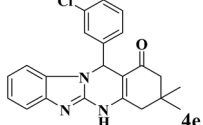
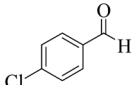
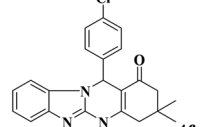
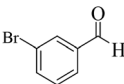
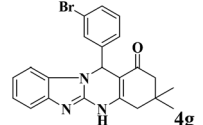
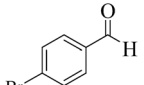
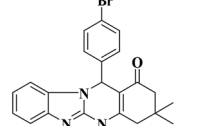
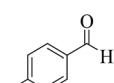
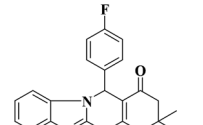
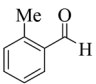
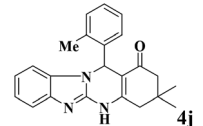
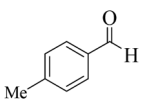
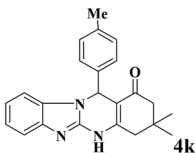
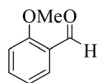
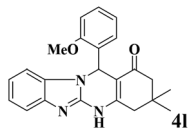
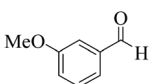
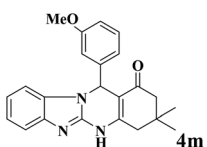
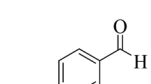
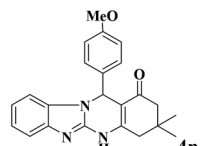
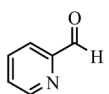
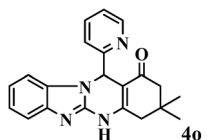
Entry	RCHO (2)	Product	Time (min)	Yield (%)	TON ^b	TOF ^c (h ⁻¹)	Mp (obsd) (°C)	Mp (lit) (°C)
1			10	94	247	1482	>350	>350 (31)
2			18	93	244	813	>300	>300 (32)
3			18	92	242	807	>350	>300 (15)
4			15	95	250	1000	>300	>300 (32)
5			15	94	247	988	>300	>300 (32)
6			12	94	247	1235	>300	>300 (33)
7			12	93	244	1220	>300	>300 (32)
8			12	95	250	1250	346–349	348–350 (34)
9			15	90	236	944	>300	>300 (33)
10			12	95	250	1250	233–235	236–238 (32)



Table 2 (Contd.)

Entry	RCHO (2)	Product	Time (min)	Yield (%)	TON ^b	TOF ^c (h ⁻¹)	Mp (obsd) (°C)	Mp (lit) (°C)
11			12	92	242	1210	240–243	242–244 (31)
12			15	90	236	944	318–322	320–323 (34)
13			20	92	242	726	318–320	320–322 (31)
14			20	90	236	708	339–342	341–343 (34)
15			15	92	242	968	338–341	337–339 (41)

^a Reaction conditions: 2-aminobenzimidazole (1 mmol), aldehyde (1 mmol), dimedone (1 mmol), Cu@Fe₃O₄ MNPs (0.38 mol%). ^b Number of moles of product produced from 1 mole of catalyst. ^c TON per unit of time.

sodium hydroxide (10%) to neutralize the excess hydrochloric acid present in the reaction vessel. Lastly, the synthesized Fe₃O₄@Gu@TSH was magnetically recycled and rinsed with ethanol several times and then dried in a vacuum oven.

Coordination of Cu(II) with Fe₃O₄@Gu@TSH. The Fe₃O₄@Gu@TSH (1 g) was distributed in 20 mL of ethanol by the ultrasonic bath for half an hour. Subsequently, CuCl₂ (2 g) was poured in to the dispersion of Fe₃O₄@Gu@TSH and the mixture was stirred for 24 hours at ambient temperature. Upon completing the reaction, the resultant precipitate Cu@Fe₃O₄ MNPs formed was separated by magnetic decantation and washed twice with ethanol (15 mL) to remove unattached metal precursors and dried under vacuum oven to afford the pure product. All stages of the Cu@Fe₃O₄ MNPs synthesis are presented in Scheme 1.

General process for the synthesis of tetrahydrobenzimidazo[2,1-*b*]quinazolin-1(2*H*)-ones (4)

A mixture of 2-aminobenzimidazole (1 mmol), aldehyde (1 mmol), dimedone (1 mmol), and Cu@Fe₃O₄ MNPs (0.38 mol%) was combined with each other at 100 °C in an oil bath under solvent-free conditions. The development of the reaction was checked

using TLC [*n*-hexane : ethyl acetate (7 : 4 ratio)] analyses. At the end of the reaction, the mixture was dissolved in a hot mixture of ethyl acetate and ethanol (4 : 10 ratio) and then the catalyst was removed using an appropriate magnet. The remaining mixture was cooled down to ambient temperature and the pure product was separated by filtration. Finally, the Cu@Fe₃O₄ MNPs were washed with chloroform, dried, and used directly with an insignificant decrease in its activity for at least five runs.

General process for the synthesis of 2*H*-indazolo[2,1-*b*]phthalazine-triones (6)

A mixture of phthalhydrazide (1 mmol), aldehyde (1 mmol), dimedone (1 mmol), and Cu@Fe₃O₄ MNPs (0.38 mol%) was combined with each other at 100 °C in an oil bath under solvent-free conditions. The progress of the reaction was monitored by TLC [*n*-hexane : ethyl acetate (7 : 4 ratio)] analyses. After completion of the reaction, the mixture was dissolved in a hot mixture of ethyl acetate and ethanol (4 : 10 ratio) and then the catalyst was removed by an external magnet. The remaining mixture was cooled to room temperature and the pure product was separated by filtration. Finally, the Cu@Fe₃O₄ MNPs were washed with chloroform, dried, and used directly with a negligible reduction of its activity for at least five runs.



Results and discussion

Catalyst characterization

FTIR analysis of Cu@MNPs. The FT-IR spectra corresponding to the Fe_3O_4 , $\text{Fe}_3\text{O}_4/\text{SiO}_2$, $\text{Fe}_3\text{O}_4/\text{PC}$, $\text{Fe}_3\text{O}_4/\text{Gu@TSH}$, $\text{Cu@Fe}_3\text{O}_4$ MNPs and recovered $\text{Cu@Fe}_3\text{O}_4$ MNPs are shown in Fig. 1. The FT-IR spectrum of the Fe_3O_4 showed characteristic absorption at 579 and 3395 cm^{-1} due to Fe–O–Fe and O–H stretching vibrations, respectively. In the spectrum of $\text{Fe}_3\text{O}_4/\text{SiO}_2$, the associated absorption bands of the Si–O–Si and Si–OH stretching vibrations were observed at 957 cm^{-1} and 1042 cm^{-1} , respectively. The FT-IR spectrum of the $\text{Fe}_3\text{O}_4/\text{PC}$ exhibits a peak at 2982 cm^{-1} that is indexed to the C–H stretching vibration mode. In $\text{Fe}_3\text{O}_4/\text{Gu@TSH}$ and $\text{Cu@Fe}_3\text{O}_4$ MNPs, the absorption peaks at 2573 cm^{-1} and 3315 cm^{-1} are indexed to the S–H and N–H stretching vibrations, respectively. Also, the peak at 1638 cm^{-1} is related with the =NH and –NH stretching vibrations of the functional groups on the surface of the Fe_3O_4 . It is necessary to mention that the spectrum of recovered $\text{Cu@Fe}_3\text{O}_4$ MNPs after the first recovery and reuse do not show any difference.

Thermal analysis of Cu@MNPs. Thermogravimetric analysis (TGA) spectrum of Fe_3O_4 , $\text{Fe}_3\text{O}_4/\text{PC}$, and $\text{Cu@Fe}_3\text{O}_4$ MNPs is presented in Fig. 2. TGA data for Fe_3O_4 and $\text{Fe}_3\text{O}_4/\text{PC}$ samples show that approximately 2% and 3.5% mass loss at

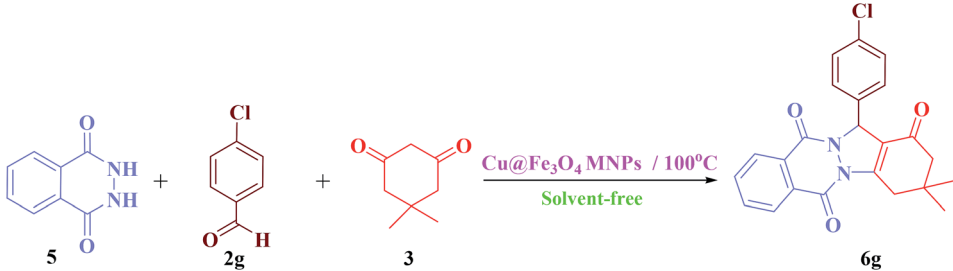
a temperature up to 600 $^\circ\text{C}$ is because of losing water molecules. The TGA curve of $\text{Cu@Fe}_3\text{O}_4$ MNPs shows two distinct steps of mass loss. The early mass loss of the $\text{Cu@Fe}_3\text{O}_4$ MNPs was less than about 200 $^\circ\text{C}$, which is due to evaporation of adsorbed water. The second significant mass loss is at temperatures within the range of 370–420 $^\circ\text{C}$, which can be related to the organic parts decomposition.

VSM analysis of Cu@MNPs. To describe the magnetic feature of the catalyst, magnetic measurements of the Fe_3O_4 and $\text{Cu@Fe}_3\text{O}_4$ MNPs were surveyed with a vibrating sample magnetometer (VSM) at ambient temperature with the field sweeping from –8500 to +8500 oersted (Fig. 3). The saturation magnetization (M_s) value of Fe_3O_4 was about 60.39 emu g^{-1} , which decreased to 33.85 emu g^{-1} because of the creation of a nonmagnetic silica shell and organic groups around the Fe_3O_4 core.

SEM analysis of Cu@MNPs. A morphological property of $\text{Cu@Fe}_3\text{O}_4$ MNPs was evaluated using SEM as shown in Fig. 4. The size of magnetite nanocatalyst was in the range 50–65 nm based on SEM measurements and has more porous surface. It illustrates that the incorporation of magnetic nanoparticles with organic groups increases surface porosity.

EDX analysis of Cu@MNPs. The energy dispersive X-ray analysis (EDX) spectrum of $\text{Cu@Fe}_3\text{O}_4$ MNPs illustrates the presence of all of the expected elements (Fe, O, Si, C, N, and Cu)

Table 3 Optimization of the three-component reaction of phthalhydrazide (5), 4-chlorobenzaldehyde (2g), and dimedone (3) under various conditions^a



Entry	Solvent	Catalyst (mol%)	Temp.	Time (min)	Yield ^b (%)
1	CH_3CN	$\text{Cu@Fe}_3\text{O}_4$ MNPs/0.38	Reflux	70	63
2	<i>n</i> -Hexane	$\text{Cu@Fe}_3\text{O}_4$ MNPs/0.38	Reflux	120	Trace
3	H_2O	$\text{Cu@Fe}_3\text{O}_4$ MNPs/0.38	Reflux	60	33
4	EtOH	$\text{Cu@Fe}_3\text{O}_4$ MNPs/0.38	Reflux	60	64
5	Solvent-free	$\text{Cu@Fe}_3\text{O}_4$ MNPs/0.38	25 $^\circ\text{C}$	12	Trace
6	Solvent-free	$\text{Cu@Fe}_3\text{O}_4$ MNPs/0.38	80 $^\circ\text{C}$	12	79
7	Solvent-free	$\text{Cu@Fe}_3\text{O}_4$ MNPs/0.38	90 $^\circ\text{C}$	12	90
8	Solvent-free	$\text{Cu@Fe}_3\text{O}_4$ MNPs/0.38	100 $^\circ\text{C}$	12	96
9	Solvent-free	$\text{Cu@Fe}_3\text{O}_4$ MNPs/0.38	110 $^\circ\text{C}$	12	93
10	Solvent-free	$\text{Cu@Fe}_3\text{O}_4$ MNPs/0.19	100 $^\circ\text{C}$	12	71
11	Solvent-free	$\text{Cu@Fe}_3\text{O}_4$ MNPs/0.57	100 $^\circ\text{C}$	12	94
12	Solvent-free	Fe_3O_4 /0.38	100 $^\circ\text{C}$	80	26
13	Solvent-free	$\text{Fe}_3\text{O}_4/\text{SiO}_2$ /0.38	100 $^\circ\text{C}$	65	37
14	Solvent-free	$\text{Fe}_3\text{O}_4/\text{PC}$ /0.38	100 $^\circ\text{C}$	60	45
15	Solvent-free	$\text{Fe}_3\text{O}_4/\text{Gu}$ /0.38	100 $^\circ\text{C}$	45	69
16	Solvent-free	$\text{Fe}_3\text{O}_4/\text{Gu@TSH}$ /0.38	100 $^\circ\text{C}$	25	85

^a Reaction conditions: phthalhydrazide (1 mmol), 4-chlorobenzaldehyde (1 mmol), dimedone (1 mmol), and the required level of the catalysts.

^b The yields refer to the isolated product.



Table 4 Cu@Fe₃O₄ MNPs-catalyzed synthesis of 2*H*-indazolo[2,1-*b*]phthalazine-trione (**6**) derivatives^a

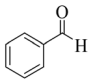
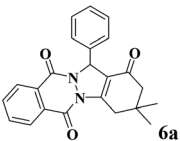
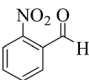
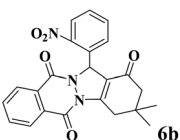
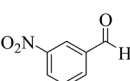
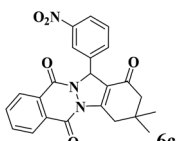
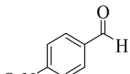
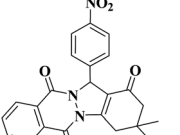
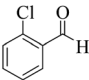
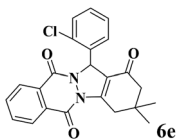
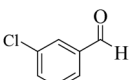
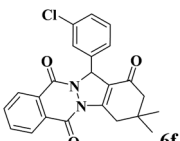
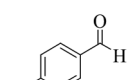
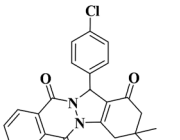
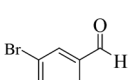
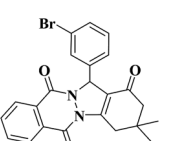
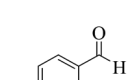
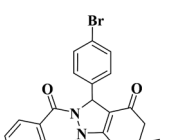
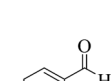
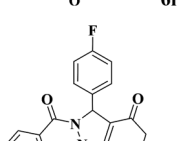
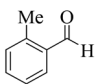
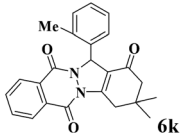
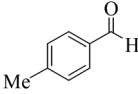
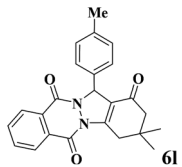
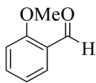
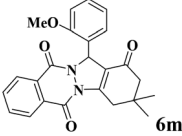
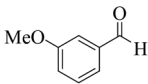
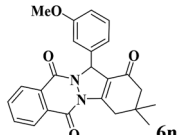
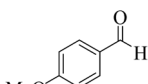
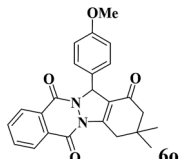
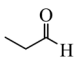
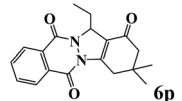
Entry	RCHO (2)	Product	Time (min)	Yield (%)	TON ^b	TOF ^c (h ⁻¹)	Mp (obsd) (°C)	Mp (lit) (°C)
1			12	95	250	1250	232–234	234–235 (36)
2			18	92	242	807	216–219	214–216 (35)
3			15	93	245	980	216–219	214–216 (37)
4			15	91	239	956	180–182	179–180 (37)
5			15	91	239	956	207–210	198–200 (37)
6			15	93	245	980	212–214	215–217 (15)
7			12	96	253	1265	212–214	215–217 (36)
8			12	93	245	1225	208–211	207–209 (35)
9			12	95	250	1250	208–211	207–209 (35)
10			12	91	239	1195	208–211	207–209 (36)



Table 4 (Contd.)

Entry	RCHO (2)	Product	Time (min)	Yield (%)	TON ^b	TOF ^c (h ⁻¹)	Mp (obsd) (°C)	Mp (lit) (°C)
11			15	91	239	956	225–229	227–230 (37)
12			15	93	245	980	217–220	220–222 (36)
13			18	91	239	797	203–205	201–202 (35)
14			18	95	250	833	223–225	224–226 (37)
15			20	93	245	735	237–239	238–240 (36)
16			35	81	213	365	146–149	145–147 (42)

^a Reaction conditions: phthalhydrazide (1 mmol), aldehyde (1 mmol), dimedone (1 mmol), Cu@Fe₃O₄ MNPs (0.38 mol%). ^b Number of moles of product produced from 1 mole of catalyst. ^c TON per unit of time.

and confirms immobilization of copper(II) complex on the Fe₃O₄ surface (Fig. 5).

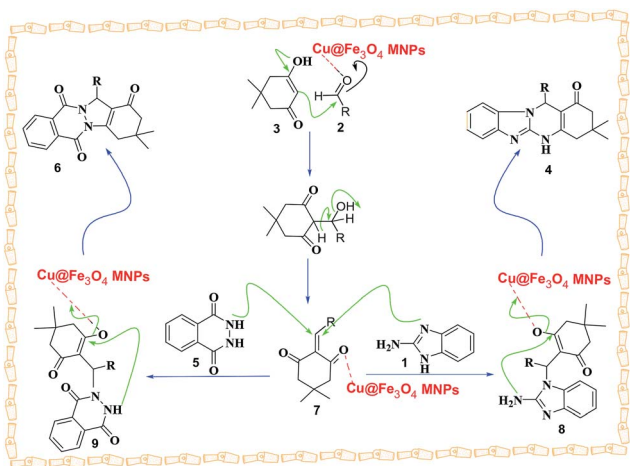
XRD analysis of Cu@MNPs. The energy dispersive X-ray analysis (EDX) spectrum of the Fe₃O₄, Fe₃O₄@Gu@TSH and Cu@Fe₃O₄ MNPs (Fig. 6) had six characteristic peaks at $2\theta = 30.29, 35.34, 43.73, 54.45, 57.51, 63.19$, and 74.58 were indexed to the (220), (311), (400), (422), (511), and (440) planes, respectively, which have a good accordance with the spinel phase of magnetic iron oxide nanoparticles. These indicated that the surface modification of the Fe₃O₄ magnetic nanoparticles with functional groups did lead to retention of the crystalline structure.

Herein, we reported our outcomes for the effective and rapid preparation of tetrahydrobenzimidazo[2,1-*b*]quinazolin-1(2*H*)-ones and 2*H*-indazolo[2,1-*b*]phthalazine-triones using an effective and reusable heterogeneous nanomagnetic catalyst, Cu@Fe₃O₄ MNPs, under solvent-free conditions (Scheme 2).

After synthesizing and identifying the Cu@Fe₃O₄ MNPs, in order to screen the reaction conditions for synthesizing

tetrahydrobenzimidazo[2,1-*b*]quinazolin-1(2*H*)-ones, the impact of the solvents, the reaction temperature, and the concentrations of catalyst were explored using the reaction of 2-aminobenzimidazole (1 mmol), 4-chlorobenzaldehyde (1 mmol) and dimedone (1 mmol) (molar ratio: 1 : 1 : 1) as a model reaction. The outcomes are listed in Table 1. To attain the optimal reaction solvent, different solvents such as CH₃CN, *n*-hexane, H₂O, and EtOH in the existence of a certain concentrations of catalyst were examined (Table 1, entries 1–4) and most favorable conditions in terms of rate and yield were found under solvent-free conditions for the reaction (Table 1, entry 8). To explore the impact of reaction temperature, different temperatures (25, 80, 90, 100, and 110 °C) were used for comparing the reaction efficiency (Table 1, entries 5–9). In the absence of temperature, the reaction speed was very slow and the yield was negligible (Table 1, entry 5). The product yield was increased at higher temperatures (Table 1, entries 6–9). At 100 °C, under solvent-free conditions, the reaction rate was the maximum (Table 1, entry 8); however, a further increase in





Scheme 3 A plausible mechanism for the creation of tetrahydrobenzimidazo[2,1-*b*]quinazolin-1(2*H*)-ones and 2*H*-indazolo[2,1-*b*]phthalazine-triones in the existence of Cu@Fe₃O₄ MNPs under solvent-free conditions.

temperature did not indicate any sign of the enhancement (Table 1, entry 9). In the following phase of the study, the impact of catalyst loading on the completion of the reaction was investigated (Table 1, entries 8 and 10–11). The outcomes indicated that the reaction using 0.38 mol% of the Cu@Fe₃O₄ MNPs as the catalyst at 100 °C under solvent-free conditions proceeded with the highest yield at the short reaction time (Table 1, entry 8). Finally, when the model reaction was performed in the presence of 0.38 mol% of Fe₃O₄, Fe₃O₄@SiO₂, Fe₃O₄@PC, Fe₃O₄@Gu, and Fe₃O₄@Gu@TSH, under the optimized conditions, the yield of the product were 43, 51, 59, 71 and 83%, respectively (Table 1, entries 12–16). The favourable comparison of the product yields for inputs 8 and 12–16 accurately exhibits that the catalyst activity increases when Fe₃O₄@Gu@TSH is coordinate to the CuCl₂ through the nitrogen lone pair.

Encouraged by these results, the scope and generality of the developed protocol regarding diverse aromatic and heterocyclic aldehydes were surveyed in the existence of 0.38 mol% of Cu@Fe₃O₄ MNPs at 100 °C under solvent-free conditions. The outcomes are presented in Table 2.

We also report a rapid and efficient one-pot three-component preparation of some 2*H*-indazolo[2,1-*b*]phthalazine-triones *via* the reaction of phthalhydrazide, aromatic aldehydes, and dimedone in the existence of Cu@Fe₃O₄ MNPs (Table 3). To identify the best conditions, we carried out the reaction between 4-chlorobenzaldehyde (1 mmol), dimedone (1 mmol) and phthalhydrazide (1 mmol) (molar ratio: 1 : 1 : 1) in the existence of 0.38 mol% of Cu@Fe₃O₄ MNPs at 100 °C under solvent-free conditions. We found that the desired product with a very high yield (96%) within 15 min (Table 3, entry 8).

After optimization of the conditions for the model reaction, a range of different tetrahydrobenzimidazo[2,1-*b*]quinazolin-1(2*H*)-ones was synthesized with array of arylaldehydes bearing either electron-withdrawing or electron-donating substituents and aliphatic aldehyde by this protocol (Table 4).

A possible mechanism for the creation of tetrahydrobenzimidazo[2,1-*b*]quinazolin-1(2*H*)-ones and 2*H*-indazolo[2,1-*b*]phthalazine-triones is proposed in Scheme 3. The reaction occurs *via* initial formation of the heterodyne 7 by nucleophilic addition of dimedone 3 to aldehyde 2 followed by dehydration. The second step involves initial formation of intermediates 8 and 9 by Michael-type addition of the 2-aminobenzimidazole 1 and phthalhydrazide 5 with heterodyne 7, followed by cyclization of the corresponding products 4 and 6.

To obtain the degree of leaching of the copper from the heterogeneous catalyst, in a typical experiment, phthalhydrazide (1 mmol), 4-chlorobenzaldehyde (1 mmol), dimedone (1 mmol), and Cu@Fe₃O₄ MNPs (0.38 mol%) and 3 mL of EtOH were placed in a round bottom flask and stirred at 100 °C for 30 min. Then, the catalyst was separated by a prominent magnetic field and allowed to the residue solution to be stirred at 100 °C for further 60 min. This experiment illustrated only a little progress in the yield of the product (GC) in the absence of Cu@Fe₃O₄ MNPs, which corroborates little leaching of copper and confirms responsibility of the heterogeneous Cu@Fe₃O₄ MNPs in catalyzing the desired reaction.

To evaluate the recycled Cu@Fe₃O₄ MNPs performance, this nanocatalyst was reused in the reaction of 2-aminobenzimidazole/phthalhydrazide with 4-hydroxy-ycoumarin, 4-chlorobenzaldehyde, and dimedone for at least

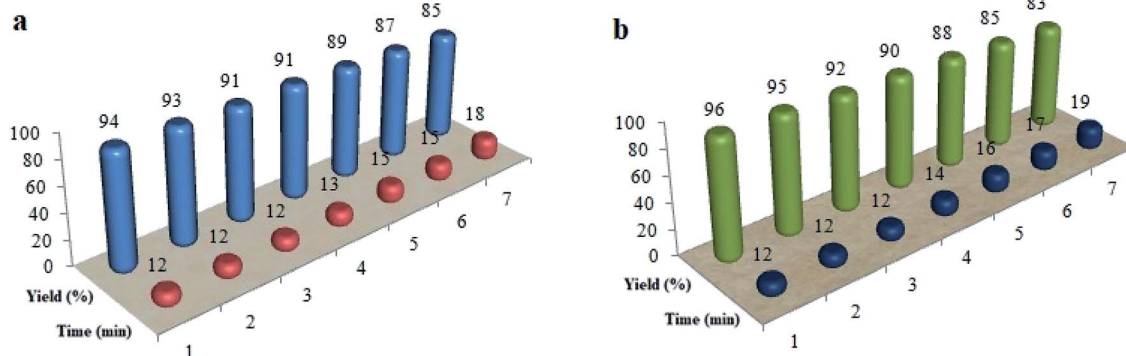


Fig. 7 The recycling of Cu@Fe₃O₄ MNPs in the preparation of tetrahydrobenzimidazo[2,1-*b*]quinazolin-1(2*H*)-ones (a) and 2*H*-indazolo[2,1-*b*]phthalazine-triones (b).

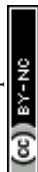
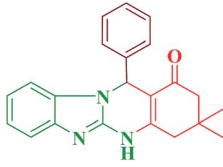
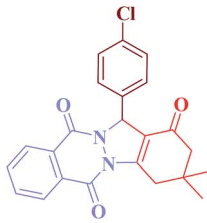


Table 5 Comparison of the current methods with other reported strategies for synthesizing tetrahydrobenzimidazo[2,1-*b*]quinazolin-1(2*H*)-ones and 2*H*-indazolo[2,1-*b*]phthalazine-triones

Entry	Catalyst	Catalyst loading	Conditions	Temp. (°C)	Time (min)	Yield (%)	Ref.
							
1	H ₆ P ₂ W ₁₈ O ₆₂ ·18H ₂ O	0.01 equiv.	CH ₃ CN	Reflux	15	96	15
2	P-TsOH·H ₂ O	15 mol%	CH ₃ CN	40–50	25	95	33
3	NH ₂ SO ₃ H	0.05 mmol	CH ₃ CN	Reflux	15	96	38
4	Iodine	10 mol%	CH ₃ CN	Reflux	10	84	14
5	Guanidinium chloride	10 mol%	Solvent-free	110	30	91	39
6	Cu@Fe ₃ O ₄ MNPs	0.38 mol%	Solvent-free	100	12	94	This work
							
1	CAN	5 mol%	PEG 400	50	120	90	24
2	Iodine	0.1 g	Sonic bath	25–30	10	92	27
3	[PVP-SO ₃ H]Cl (HMT)	8 mol%	Solvent-free	80	25	92	31
4	H ₂ SO ₄	0.15 mmol	[bmim]BF ₄	80	30	88	25
5	Mg (HSO ₄) ₂	10 mol%	Solvent-free	100	4	88	40
6	Cu@Fe ₃ O ₄ MNPs	0.38 mol%	Solvent-free	100	12	96	This work

seven runs under the optimal reaction conditions (Fig. 7). To achieve this purpose, at the end of the reaction, the mixture was dissolved in a hot mixture of ethyl acetate and ethanol (4 : 10 ratio) and then the catalyst was removed using an appropriate magnet. The recovered Cu@Fe₃O₄ MNPs were washed with chloroform, dried, and reused with a negligible reduction of its activity.

Table 5 shows the efficiency of Cu@Fe₃O₄ MNPs as the catalyst in the preparation of tetrahydrobenzimidazo[2,1-*b*]quinazolin-1(2*H*)-ones and 2*H*-indazolo[2,1-*b*]phthalazine-triones compared with several of the previously mentioned homogeneous and heterogeneous catalysts. As clearly shown in Table 5, although all the reported catalysts are suitable for certain synthetic conditions, the catalytic behavior of the present catalytic system is remarkable in terms of low reaction times, easy work-up procedures, low catalyst loading, and simple recovery of the catalyst.

Conclusion

In summary, a novel, effective, and recyclable nanocatalyst, *i.e.*, Cu@Fe₃O₄ MNPs, was prepared, characterized, and verified in terms of its catalytic activity. Cu@Fe₃O₄ MNPs was proven to be an eco-friendly environment for the preparation of tetrahydrobenzimidazo[2,1-*b*]quinazolin-1(2*H*)-ones and 2*H*-indazolo[2,1-*b*]phthalazine-triones *via* two one-pot three-component

condensations under solvent-free conditions. This method provides several advantages including applying a green catalyst, lower loading of the catalyst, magnetically separable, omitting organic solvent, simple operation, and good to high yields.

Conflicts of interest

There are no conflicts to declare.

Acknowledgements

This investigation has been supported by the Guangxi Natural Science Foundation (No. 2018JJA120123).

References

- 1 B. M. Trost, *Science*, 1991, **254**, 1471.
- 2 M. Valden, X. Lai and D. W. Goodman, *Science*, 1998, **281**, 1647.
- 3 G. Hutchings, *Nanocatalysis: Synthesis and Applications*, ed. V. Polshettiwar and T. Asefa, John Wiley & Sons, 2013.
- 4 D. J. Cole-Hamilton, *Science*, 2003, **299**, 1702.
- 5 R. J. White, R. Luque, V. L. Budarin, J. H. Clark and D. J. Macquarrie, *Chem. Soc. Rev.*, 2009, **38**, 481.
- 6 A. C. Templeton, M. J. Hostetler, E. K. Warmoth, S. Chen, C. M. Hartshorn, V. M. Krishnamurthy, M. D. Forbes and R. W. Murray, *J. Am. Chem. Soc.*, 1998, **120**, 4845.



- 7 J. A. Gladysz, *Chem. Rev.*, 2002, **102**, 3215.
- 8 A. Zecchina, S. Bordiga and E. Groppo, *Selective Nanocatalysts and Nanoscience: Concepts for Heterogeneous and Homogeneous Catalysis*, John Wiley & Sons, 2011.
- 9 V. Alagarsamy and U. S. Pathak, *Bioorg. Med. Chem.*, 2007, **15**, 3457.
- 10 V. Alagarsamy, *Pharmazie*, 2004, **59**, 753.
- 11 V. Alagarsamy, G. Murugananthan and R. Venkateshperumal, *Biol. Pharm. Bull.*, 2003, **26**, 1711.
- 12 M. J. Hour, L. J. Huang, S. C. Kuo, Y. Xia, K. Bastow, Y. Nakanishi, E. Hamel and K. H. Lee, *J. Med. Chem.*, 2000, **43**, 4479.
- 13 V. Alagarsamy, R. Revathi, S. Meena, K. V. Ramaseshu, S. Rajasekaran and E. De Clercq, *Indian J. Pharm. Sci.*, 2004, **66**, 459.
- 14 R. G. Puligoundla, S. Karnakanti, R. Bantu, N. Kommu, S. B. Kondra and L. Nagarapu, *Tetrahedron Lett.*, 2013, **54**, 2480.
- 15 M. M. Heravi, L. Ranjbar, F. Derikvand, B. Alimadadi, H. A. Oskooie and F. F. Bamoharram, *Mol. Diversity*, 2008, **12**, 181.
- 16 G. M. Ziarani, A. Badiei, Z. Aslani and N. Lashgari, *Arabian J. Chem.*, 2015, **8**, 54.
- 17 G. Krishnamurthy and K. V. Jagannath, *J. Chem. Sci.*, 2013, **125**, 807.
- 18 A. E. Mourad, A. A. Aly, H. H. Farag and E. A. Beshr, *Beilstein J. Org. Chem.*, 2007, **3**, 1.
- 19 J. Li, Y. F. Zhao, X. Y. Yuan and J. X. Xu, *Molecules*, 2006, **11**, 574.
- 20 C. K. Ryu, R. E. Park, M. Y. Ma and J. H. Nho, *Bioorg. Med. Chem. Lett.*, 2007, **17**, 2577.
- 21 N. Watanabe, Y. Kabasawa, Y. Takase, M. Matsukura, K. Miyazaki, H. Ishihara, K. Kodama and H. Adachi, *J. Med. Chem.*, 1998, **41**, 3367.
- 22 S. Grasso, G. DeSarro, N. Micale, M. Zappala, G. Puia, M. Baraldi and C. Demicheli, *J. Med. Chem.*, 2000, **43**, 2851.
- 23 Y. Nomoto, H. Obase, H. Takai, M. Teranishi, J. Nakamura and K. Kubo, *Chem. Pharm. Bull.*, 1990, **38**, 2179.
- 24 K. Mazaahir, C. Ritika and J. Anwar, *Chin. Sci. Bull.*, 2012, **57**, 2273.
- 25 J. M. Khurana and D. Magoo, *Tetrahedron Lett.*, 2009, **50**, 7300.
- 26 B. Dam, M. Saha, R. Jamatia and A. K. Pal, *RSC Adv.*, 2016, **6**, 54768.
- 27 A. Varghese, A. Nizam, R. Kulkarni and L. George, *Eur. J. Chem.*, 2013, **4**, 132.
- 28 X. N. Zhao, G. F. Hu, M. Tang, T. T. Shi, X. L. Guo, T. T. Li and Z. H. Zhang, *RSC Adv.*, 2014, **4**, 51089.
- 29 H. R. Shaterian, M. Ghashang and M. Feyzi, *Appl. Catal., A*, 2008, **345**, 128.
- 30 A. R. Kiasat, S. Noorizadeh, M. Ghahremani and S. J. Saghanejad, *J. Mol. Struct.*, 2013, **1036**, 216.
- 31 O. G. Jolodar, F. Shirini and M. Seddighi, *RSC Adv.*, 2016, **6**, 44794.
- 32 A. Shaabani, E. Farhangi and A. Rahmati, *Comb. Chem. High Throughput Screening*, 2006, **9**, 771.
- 33 M. R. Mousavi and M. T. Maghsoudlou, *Monatsh. Chem.*, 2014, **145**, 1967.
- 34 F. Shirini, M. Seddighi and O. G. Jolodar, *J. Iran. Chem. Soc.*, 2016, **13**, 1077.
- 35 F. Shirini, M. S. N. Langarudi and O. G. Jolodar, *Dyes Pigm.*, 2015, **123**, 186.
- 36 B. Mombani Godajdar, A. R. Kiasat and M. M. Hashemi, *Heterocycles*, 2013, **87**, 559.
- 37 A. Rostami, B. Tahmasbi and A. Yari, *Bull. Korean Chem. Soc.*, 2013, **34**, 1521.
- 38 M. M. Heravi, F. Derikvand and L. Ranjbar, *Synth. Commun.*, 2010, **40**, 677.
- 39 R. Talaei and A. Olyaei, *Iran. J. Catal.*, 2016, **6**, 339.
- 40 H. R. Shaterian, F. Khorami, A. Amirzadeh, R. Doostmohammadi and M. Ghashang, *Journal of the Iranian Chemical Research*, 2009, **2**, 57.
- 41 M. Dehghan, A. Davoodnia, M. R. Bozorgmehr and F. F. Bamoharram, *Org. Prep. Proced. Int.*, 2017, **49**, 236.
- 42 R. G. Vaghei, R. Karimi-Nami, Z. Toghræi-Semiromi, M. Amiri and M. Ghavidel, *Tetrahedron*, 2011, **67**, 1930.

